J. Dairy Sci. 107:8609–8628
https://doi.org/10.3168/jds.2024-24809

Cyclical heat stress during lactation influences the microstructure of the bovine mammary gland

G. Perez-Hernandez,[1] M. D. Ellett,[1] L. J. Banda,[2] D. Dougherty,[1] C. L. M. Parsons,[1] A. J. Lengi,[1] K. M. Daniels,[1] and B. A. Corl[1]*
[1]School of Animal Sciences, Virginia Tech, Blacksburg, VA 24061
[2]Animal Science Department, Lilongwe University of Agriculture and Natural Resources, Lilongwe, Malawi

ABSTRACT

This study aimed to evaluate the effect of heat stress on mammary epithelial cell (MEC) losses into milk, secretory mammary tissue structure, and mammary epithelial cell activity. Sixteen multiparous Holstein cows (632 ± 12 kg BW) approximately 100 DIM housed in climate-controlled rooms were paired by BW and randomly allocated to one of 2 treatments, heat stress (HS) or pair-feeding thermoneutral (PFTN) using 2 cohorts. Each cohort was subjected to 2 periods of 4 d each. In period 1, both treatments had ad libitum access to a common TMR and were exposed to a controlled daily temperature-humidity index (THI) of 64. In period 2, HS cows were exposed to controlled cyclical heat stress (THI: 74–80), while PFTN cows remained at 64 THI and daily DMI was matched to that of the HS cows. Cows were milked twice daily, and milk yield was recorded at each milking. Individual milk samples on the last day of each period were used to quantify MEC losses by flow cytometry using butyrophilin as a cell surface marker. On the final day of period 2, individual bovine mammary tissue samples were obtained for histomorphology analysis, assessment of protein abundance, and evaluation of gene expression of targets associated with cellular capacity for milk and milk component synthesis, heat response, cellular proliferation, and autophagy. Statistical analysis was performed using the GLIMMIX procedure of SAS. Milk yield was reduced by 4.3 kg by HS (n = 7) compared with PFTN (n = 8). Independent of treatment, MEC in milk averaged 174 cells/mL (2.9% of total cells). There was no difference between HS and PFTN cows for MEC shed or concentration in milk. Alveolar area was reduced 25% by HS, and HS had 4.1 more alveoli than PFTN. The total number of nucleated MEC per area was greater in HS cows (389 ± 1.05; mean ± SE) compared with PFTN (321 ± 1.05); however, cell number per alveolus was similar between groups (25 ± 1.5 vs. 26 ± 1.4). There were no differences in relative fold expression for *GLUT1*, *GLUT8*, *CSN2*, *CSN3*, *LALBA*, *FASN*, *HSPA5*, and *HSPA8* in HS cows compared with PFTN cows. Immunoblotting analyses showed a decrease in abundance for phosphorylated STAT5 and S6K1, and an increase in LC3 II in HS cows compared with PFTN cows. These results suggest that even if milk yield differences and histological changes occur in the bovine mammary gland after 4 d of heat exposure, MEC loss into milk, nucleated MEC number per alveolus, and gene expression of nutrient transport, milk component synthesis, and heat-stress-related targets are unaffected. In contrast, the abundance of proteins related to protein synthesis and cell survival decreased significantly, whereas proteins associated with autophagy were upregulated in HS cows compared with PFTN cows.
Key words: mammary gland structure, MEC loss and number, heat stress, lactation

INTRODUCTION

Heat is an environmental threat to dairy farms. Dairy cows are homeothermic animals that express their maximum genetic merit and production capacity within a demarcated thermoneutral zone. The thermoneutral zone is the range in which organisms maintain physiological homeostasis by regulating heat loss without altering metabolic heat production (Blatteis et al., 2001). However, temperature is not the only factor determining the apparent or perceived temperature. Perceived temperature results from combined meteorological factors such as air temperature and relative humidity, and it is reflected by the temperature and humidity index (**THI**) with an inherent THI limit that high-producing dairy cows can tolerate. In dairy cows, the THI threshold is about 68 (Ravagnolo et al., 2000; Zimbelman et al., 2011; Fabris et al., 2019), and the initiation of a heat stress (**HS**) response in the cow is triggered when this THI threshold is exceeded.

Received February 20, 2024.
Accepted April 19, 2024.
*Corresponding author: bcorl@vt.edu

The list of standard abbreviations for JDS is available at adsa.org/jds-abbreviations-24. Nonstandard abbreviations are available in the Notes.

The remarkable economic (St-Pierre et al., 2003; Key et al., 2014) and physiological effects of heat stress in livestock and dairy cattle have been broadly studied in the past decade (Zimbelman et al., 2009; Wheelock et al., 2010; Baumgard and Rhoads, 2013). One of the major HS responses described in dairy cattle is milk yield (**MY**) reduction and milk component alteration. The use of pair-feeding studies has shown that around 50% of the milk production reduction during HS occurs due to the associated decrease in daily DMI (Wheelock et al., 2010; Cowley et al., 2015; Gao et al., 2017). Nevertheless, the remaining causative mechanisms of MY deterioration during HS independent of DMI reduction have not been fully elucidated.

The mammary gland produces milk through secretory mammary epithelial cells (**MEC**). The number and activity level of epithelial cells are determining factors of synthetic and secretory abilities within each mammary gland, and consequently, milk production (Capuco et al., 2001, 2003). Potential effects on metabolic and physiological alterations of MEC that affect intracellular signaling pathways involved in productivity have been suggested. As reviewed by Sonna et al. (2002), the effects of HS on mammalian cells encompass disruptions in fundamental cellular processes at gene (DNA synthesis, RNA transcription and translation) and protein level (protein degradation, denaturation, and misaggregation). These disruptions lead to cell-cycle arrest, alterations in cell metabolism resulting in a decrease in cellular ATP, as well as disruptions in cytoskeletal components and membrane permeability.

The aforementioned effects have been evaluated using in vitro (Collier et al., 2008) and in vivo models (Silanikove et al., 2009; Baumgard and Rhoads, 2012). Several studies have explored HS effects on the mammary gland during the dry period (Tao et al., 2011; Dado-Senn et al., 2019; Fabris et al., 2020); however, the effects of HS on the bovine mammary gland during lactation, beyond noting lowered milk production and alterations to composition, have not been extensively characterized. We hypothesized that HS specifically alters MEC numbers and cell losses into milk and, more generally, affects mammary cellular activity. Therefore, using a pair-feeding model, the objective of this study was to evaluate the effect of HS on the mammary gland related to cell number and activity and cell losses in milk of lactating Holstein cows.

MATERIALS AND METHODS

Animals, Experimental Design, and Treatments

The use of animals and all procedures for this investigation were approved by the Virginia Tech Institutional Animal Care and Use Committee (19-247). Sixteen lactating multiparous Holstein cows (100 ± 14 DIM; 632 ± 12 kg BW) were used in the study. All cows enrolled in the experiment were visually free of diseases. The trial was conducted from May to August 2021 and the overall experiment was performed using 2 cohorts with 8 cows per cohort. Cows were housed in 2 individual climate-controlled rooms at the Metabolic Research Laboratory at the Virginia Tech Dairy Farm (Blacksburg, VA) throughout the experiment. Upon arrival at the climate-controlled facilities, cows were moved to individual tiestalls within one of 2 climate-controlled rooms, received a common TMR for ad libitum intake and allowed to acclimate for 4 (HS group) and 5 (pair-feeding thermoneutral [**PFTN**] group) days under thermoneutral conditions, consisting of a THI of 64. The difference in enrollment time between groups was intentionally set to establish a one-day lag, enabling pair-feeding intake. Milk yield and DMI were recorded during this time to monitor health status and cow adaptation response, but no data were included in the experiment analyses. During the adaptation period, one cow from the HS treatment had to be removed from the experiment before treatment imposition due to health problems unrelated to the trial.

On the last day of acclimation cows were assigned to one of 2 treatments: HS (n = 7) or PFTN (n = 8). The experiment had 2 periods that lasted 4 d each. During period 1, both treatments had ad libitum access to a common TMR and were exposed to a daily THI of 64. In period 2, HS cows were exposed to cyclical heat stress with daily THI from 74 (1800–0600 h) to 80 (0600–1800 h) and PFTN cows remained at a THI of 64.

Throughout the experiment, each cow was tethered in a tiestall bedded with sawdust shavings and the lighting regimen consisted of a 16 h light cycle followed by an 8 h dark cycle. The cows were fed a complete TMR, formulated according to the nutritional guidelines outlined by the National Research Council (NRC, 2001), twice daily at 0900 and 1900 h. For ingredient and nutrient composition of diets, review Ellett et al. (2024). Daily feed intake was paired using as reference the day-before intake from the HS group during period 2. Continuous access to clean water was provided to all cows. Milking sessions were set daily at 0700 and 1900 h and cows were milked in their individual tiestalls. Individual feed intake, cow vital signs (rectal temperatures and respiration rates) and MY were recorded daily. The animals were housed continuously within controlled climate chambers until the time of slaughter. At the end of period 2, all cows were stunned via penetrating captive bolt and euthanized via exsanguination.

The THI was calculated using data from wireless data loggers (model number EL-USB-2+; Lascar Electronics, Whiteparish, Salisbury, UK) as THI = 0.8 × T + [RH

× (T − 14.4)] + 46.4; where T = mean hourly ambient temperature in °C and RH = mean hourly relative humidity divided by 100. For a complete description of the experimental design and associated results see Ellett et al. (2024).

Milk Sample Collection and Flow Cytometry Analysis

Epithelial and immune cells in milk were quantified by flow cytometry. For this, representative milk samples (3.8 L) from the morning milking were collected on the last day (d 4) of each period from each cow and processed according to the protocol of Lengi et al. (2021). Briefly, milk samples containing a final concentration of 0.5 m*M* EDTA were centrifuged (850 × *g* for 10 min at room temperature) to pellet the total cells present in milk. The resulting pellet was washed once with Dulbecco's PBS and EDTA (0.5 m*M* final concentration), centrifuged, resuspended for 15 min in red blood cell lysis buffer, and filtered sequentially through 100- and 40-µm sterile cell strainers (Genesee Scientific) to remove noncellular debris. Cell number was assessed using a hemocytometer and samples were adjusted to 2×10^6 cells for flow cytometry analysis. Primary cell-surface antibodies previously reported and tested for hematopoietic cells (protein tyrosine phosphatase receptor type C [**CD45**]; clone CACTB51A, Kingfisher Biotech, 3.1 ng/µL), macrophages (cluster of differentiation 14 [**CD14**]; clone CAM 36A, Kingfisher Biotech, 1.25 ng/µL), and MEC (butyrophilin 1A1 [**BTN**]; clone 2151C conjugated to APC, NOVUS Biologicals, 7 ng/µL) were used to label individual cells. Secondary antibodies used were rat anti-mouse IgG2a-phycoerythrin (clone SB84a, Southern Biotech Associates, 1.0 ng/µL) and goat anti-mouse IgG1-AlexaFluor 488 (Southern Biotech Associates, 1.25 ng/µL). Cell viability was assessed using propidium iodide (**PI**; BD Biosciences, 5 µg/mL) dye, and Hoechst 33342 (Invitrogen, 10 µg/mL) was used as a nucleic acid stain.

Flow cytometry was conducted on a BD FACSAria Fusion (BD Biosciences) using FACSDiva software (BD Biosciences). Side and forward scatter thresholds were set to exclude cellular debris and aggregates. Single stains of each fluorophore and dye were used to determine flow cytometry compensation settings. Gates were used to discriminate positive and negative staining cells and were applied consistently to all samples allowing for minor adjustments for side scatter variability. Live and nucleated cells were selected by gating on PI and Hoechst, and different subpopulations were selected by gating on cells triple-labeled with CD45-PE, CD14-AF488, and BTN-APC.

Mammary Gland Tissue Collection and Processing

Mammary tissue samples from right rear mammary glands (~100 g total, collected from midgland region) were collected within 20 min of slaughter and rinsed with cold PBS. Excised mammary tissue was then cut into smaller pieces for subsampling. Subsamples intended for histology were stored in room temperature 10% neutral buffered formalin for 24 h for fixation; samples for subsequent transcript analysis were snap-frozen in liquid nitrogen and stored at −80°C, and samples for later protein analyses were homogenized in lysis buffer and snap-frozen in liquid nitrogen and stored at −80°C.

Histological Analysis

After fixation, mammary tissue samples were subsequently stored in 70% ethanol at 4°C. Later, samples were processed using a Leica TP-1020 Tissue Processor (Leica Microsystems, Deerfield, IL), and embedded in paraffin. Embedded paraffin blocks were sliced using an HM-340E Microm GmbH microtome (Walldorf, Germany) in 5-µm-thick sections, incubated in a water bath for 5 min, and placed on positively charged microscope slides (Fisher Scientific; Pittsburgh, PA). Three tissue sections were placed on each slide with one slide per cow. Slides were placed on a slide warmer after draining to thoroughly dry. Slides were then deparaffinized, rehydrated, and stained with hematoxylin and eosin (**H&E**), and coverslipped using standard procedures.

Alveoli number, alveoli area (MEC and lumen of alveoli), and MEC number per alveolus were quantified from H&E stained slides. Histologic sections were randomly photographed using OCULAR Imaging Acquisition Software (Teledyne Photometrics, Tucson, AZ) avoiding tissue edges. Seven images from each tissue section were captured using a 20× objective for alveoli area, alveoli number, and cell number. For histological analysis, one tissue section was randomly selected, and the 7 images were evaluated for alveoli number and alveoli area. For cell number analyses, 5 images, randomly selected, were evaluated. Slide evaluation was carried out using ImageJ software (National Institutes of Health, Bethesda, MD). The ImageJ Point Picker plugin was used to count alveoli number and nucleated cells, and the alveoli area was traced using the Freehand tool. The image was calibrated according to the corresponding magnification (pixels to micrometers). Total area captured in photomicrographs taken at 20× was 304,821 μm^2. The percentage area was calculated as the portion of the alveolar area compared with the total image area. Ducts were not measured or considered in the

analysis. Alveoli number, cell number, and alveoli area were averaged across images per section for each cow for statistical analysis.

Reverse Transcription Quantitative PCR

For total RNA extraction, ~100 mg of snap-frozen tissue were homogenized in 1 mL of RNAzol RT Reagent (Molecular Research Center Inc., Cincinnati, OH) using a PRO 200 homogenizer (PRO Scientific Inc., Oxford, CT) following the manufacturer's instructions. Homogenates were centrifuged at 12,000 × *g* for 15 min at 4°C, and RNA was isolated and resuspended in nuclease-free water. The RNA concentration of each sample was determined at 260 nm using a Nano-Drop 1000 spectrophotometer (Thermo Fisher Scientific Inc., Wilmington, DE). For cDNA synthesis, total RNA (2 µg per reaction) was reverse transcribed for 1 h at 37°C using the Omniscript Reverse Transcription kit (Qiagen, Valencia, CA) according to the manufacturer's instructions. Oligo-dT (Qiagen, Valencia, CA) was used as the primer for reverse transcription. After cDNA synthesis, aliquoted samples were stored at −20°C until PCR analysis. Genes of interest were selected for analysis due to known roles in nutrient transport across MEC membranes, milk component synthesis, and cellular response to heat (Table 1).

Real-time quantitative PCR was performed using the Quantitect SYBR Green PCR kit (Qiagen) in an Applied Biosystems 7300 real-time PCR machine (Applied Biosystems, Foster City, CA). Duplicate wells were employed for each reaction using a final reaction volume of 25 µL. Each PCR reaction consisted of 2.5 µL of cDNA, 12.5 µL of SYBR Green, 2.5 µL of both reverse and forward primers, and 5 µL of RNase-free water. Amplification reactions were as follows: enzyme activation at 95°C for 10 min, followed by 40 cycles of denaturation at 95°C for 30 s, annealing at 58°C for 30 s, and elongation for 72°C for 1 min.

To define the most reliable endogenous control genes for normalization, primers for 6 different transcripts (*ACTB*, *B2M*, *EIF3K*, *MRLP39*, *RLP0*, *PPIA*) were tested to identify the most stable across samples. The stability of candidate control transcripts was analyzed and ranked using RefFinder (Xie et al., 2012) and the 2 most stable, *ACTB* and *EIF3K*, were used as the endogenous controls. Fold-change data were analyzed using the common base method (Ganger et al., 2017). All primer pairs were designed to span at least one intron and generated a single product on dissociation curve analysis. Gene-specific primers for the transcripts used in the study and their efficiencies are shown in Table 1.

Immunoblotting

Tissue samples used for immunoblotting were removed from storage at −80°C and homogenized in 2 mL of lysis buffer, 50 m*M* Tris pH 7.4, 0.5% Triton X-100, 0.3 *M* NaCl, 2 m*M* EDTA pH 8.0, 1 m*M* sodium orthovanadate, and 2% protease inhibitor cocktail (Sigma-Aldrich, Saint Louis, MO), using a homogenizer (PRO 200; Scientific Inc., Oxford, CT). Samples were always kept on ice. Before total protein quantification, tissue homogenates were centrifuged at 14,000 × *g* for 10 min at 4°C to spin down cellular debris. The resultant supernatant fractions were transferred to new tubes, and total protein concentration was assessed (Bradford Reagent; Bio-Rad, Hercules, CA). Samples were standardized to 3.4 µg total protein per microliter using Laemmli Sample Buffer (Sigma Chemical Co., St. Louis, MO) and incubated at 95°C on a heat block for 10 min. Aliquots were stored at −20°C until analysis. For immunoblot analysis, the Precision Plus Protein Kaleidoscope (Bio-Rad) was used as a molecular weight ladder, and 42.5 µg of total protein were loaded into each polyacrylamide gel well (10%, 12%, or 15%; Mini-PROTEAN TGX Stain-Free Precast; Bio-Rad) for electrophoresis according to the target protein molecular weight. Stain-free gel activation was completed using UV light and a ChemiDoc MP Imaging System (Bio-Rad) and transferred onto a mini polyvinylidene difluoride membrane (Trans-Blot Turbo RTA Transfer Kit, Bio-Rad) for 7 min using a Bio-Rad Trans-Blot Turbo semi-dry transfer apparatus (Bio-Rad). Membranes were blocked for 1 h at room temperature under slight agitation using 2% BSA in tris-buffered saline solution with Tween 20 (**TBST**; 0.05 *M* Tris pH 7.4, 0.2 *M* NaCl, 0.1% Tween) for phosphorylated target proteins or 5% nonfat dry milk in TBST for total quantification. Membranes were incubated with primary antibodies overnight at 4°C on a rocking platform. The following day membranes were washed with TBS and incubated in the corresponding horseradish peroxidase (**HRP**)-conjugated secondary antibody for 1 h on a rocking platform at room temperature. Enhanced chemiluminescence protein detection reagent was used for protein detection according to the manufacturer's protocol (Amersham ECL Prime, Cytiva, Washington, DC). The ChemiDoc MP system was used for imaging and ImageLab software (Bio-Rad) was used for densitometric analysis. Target protein band intensity was normalized by dividing the intensity of the target protein band by the intensity of the corresponding total protein in the entire lane. To evaluate cell activity, proteins of interest were selected based on known roles in cell survival, cell differentiation, and protein synthesis. Antibodies used for immunoblotting can be found in

Table 1. Gene targets, primer sequences, and efficiencies for real-time quantitative PCR[1]

Gene	Full gene name	Sequence[2] (5′ to 3′)	Length (bp)	NCBI[3] accession number	Reaction efficiency, %
Milk components					
CSN2	β-Casein	F: TGGCTCCTAAGCACAAAGAAA R: GGACTGAGAAAGGGACAGCA	150	NC_037333.1	102.4
CSN3	κ-Casein	F: AGCCCACCTGAGATCAACAC R: GCCGGATCTGTGAAAATCAT	1,987	NC_037333.1	106.4
LALBA	α-Lactalbumin	F: TACTGGTTGGCCCATAAAGC R: CAAGGGGGTACAAAGAAGCA	104	NC_037332.1	97.3
FASN	Fatty acid synthase	F: CTGCAACTCAACGGGAACTT R: AGGCTGGTCATGTTCTCCAG	102	NC_037346.1	99.6
Nutrient transport					
GLUT1	Glucose transporter 1	F: TCCTGCTCATTAACCGCAAC R: GGCTCTCCTCCTTCATCTCC	108	NC_037330.1	88.5
GLUT8	Glucose transporter 8	F: TGGCCCCGGTCTATATCTCT R: GGAGGATGCCTGTGACTACC	93	NC_037338.1	93.4
Heat stress					
HSPA5	Heat shock protein 70 A5	F: TTCCCAACATCAAGCAAGAA R: AGAGCCACCAACAAGAACAA	196	NC_037338.1	99.7
HSPA8	Heat shock protein 70 A8	F: GCATTCCAGGTTGCTGACTCT R: AATGCCAACTGCAGGTCCTT	80	NC_037342.1	99.3
Endogenous control genes					
ACTB	β-Actin	F: CTCTTCCAGCCTTCCTTCCT R: GGGCAGTGATCTCTTTCTGC	217	NM_173979.3	102.4
EIF3K	Eukaryotic translation initiation factor 3 subunit K	F: GCGATGTTTGAGCAGATGAG R: GCATTTTCTTTGGCCTGTGT	991	NM_001034489.2	97.6

[1]Amplification protocol: enzyme activation at 95°C for 10 min, 40 cycles of denaturation at 95°C for 30 s, annealing at 58°C for 30 s, and elongation for 72°C for 1 min.

[2]F = forward; R = reverse.

[3]NCBI = National Center for Biotechnology Information.

Table 2. Antibodies, protein target function, and concentrations (primary and secondary) used for immunoblotting

Primary antibody[1]	Protein symbol	Category	Primary antibody concentration	Secondary antibody concentration[2]	Company	Catalog number
Eukaryotic translation initiation factor 4E binding protein 1	4EBP1	mTOR pathway	1:1,000	1:2,000	MyBiosource.com	MBS8211698
Mammalian target of rapamycin	mTOR[3]	mTOR pathway	1:1,000	1:2,000	Cell Signaling Technology	2972
Phosphorylated mammalian target of rapamycin	pmTOR[3]	mTOR pathway	1:1,000	1:2,000	Cell Signaling Technology	S2448
Cluster of differentiation 14	CD14[3]	Innate immune system	1:5,000	1:10,000	Bio-Rad	MAC5940GA
Autophagy-related 7	ATG7	Cell survival/autophagy	1:1,000	1:2,000	Cell Signaling Technology	8558
Microtubule-associated protein 1A/1B–light chain 3–phosphatidylethanolamine conjugate	LC3 II	Cell survival/autophagy	1:500	1:20,000	Invitrogen Thermo Fisher Scientific	PA1-16930
Microtubule-associated protein 1A/1B-light chain 3	LC3 I[3]	Cell survival/autophagy	1:500	1:20,000	Invitrogen Thermo Fisher Scientific	PA5-22990
Prolactin	PRL[3]	JAK/STAT signaling pathway	1:1,000	1:2,000	Invitrogen	MBS8211698
Prolactin receptor	PRLR	JAK/STAT signaling pathway	1:1,000	1:2,000	MyBiosource.com	2026485
Protein kinase B	AKT	mTOR pathway	1:1,000	1:2,000	Cell Signaling Technology	9272
Phosphorylated protein kinase B	pAKT (Ser473)	mTOR pathway	1:1,000	1:10,000	Cell Signaling Technology	9271
Extracellular signal-regulated protein kinases 1 and 2	ERK1/2	MAPK signaling cascade	1:1,000	1:2,000	Invitrogen Thermo Fisher Scientific	MA5-15134
Phosphorylated extracellular signal-regulated protein kinases 1 and 2	pERK1/2 (Thr185, Thr187)	MAPK signaling cascade	1:1,000	1:5,000	Invitrogen Thermo Fisher Scientific	44-680G
Phosphorylated p38 mitogen-activated protein kinase	Pp38 MAPK[3]	MAPK signaling cascade	1:1,000	1:5,000	Cell Signaling Technology	4511
p38 Mitogen-activated protein kinase	p38 MAPK	MAPK signaling cascade	1:1,000	1:2,000	Cell Signaling Technology	9212
Signal transducer and activator of transcription 5	STAT5	JAK/STAT signaling pathway	1:1,000	1:2,000	Cell Signaling Technology	94205
Phosphorylated signal transducer and activator of transcription 5	pSTAT5 (Tyr694)	JAK/STAT signaling pathway	1:1,000	1:5,000	Cell Signaling Technology	9351
Ribosomal protein S6 kinase β-1	S6K1	mTOR pathway	1:1,000	1:2,000	Biorbyt	orb 30457
Phosphorylated ribosomal protein S6 kinase β-1	pS6K1 (Thr412)	mTOR pathway	1:1,000	1:2,000	LS Bioscience	C368518-30

[1]Antibodies were diluted using blocking buffer 2% BSA or 5% nonfat dry milk in 1× tris-buffered saline solution with Tween 20.

[2]Secondary antibodies used were mouse anti-rabbit IgG-HRP and goat anti-mouse IgG1-HRP (catalog nos. sc-2357 and sc-2060, Santa Cruz Biotechnology).

[3]Antibodies against CD14, LC3 I, prolactin, mTOR, pmTOR, and phosphorylated p38 MAPK did not produce detectable bands with these samples. Titration tests were conducted for all antibodies.

Table 3. Least squares means of vital signs, MY, and milk components of lactating multiparous Holstein cows following 4 d under controlled thermoneutral (pair-fed; THI of 64; n = 8) or cyclical HS conditions (THI from 74 to 80; n = 7)

Item	PFTN	HS	SEM	*P*-value[1]
Respiratory rate, breaths/min	35.25	79.75	3.02	0.0001
Rectal temperature, °C	38.6	40.0	0.10	0.0001
MY, kg/d	37.54	33.20	1.08	0.01
Protein yield, kg	1.05	0.87	0.04	0.02
Fat yield, kg	1.42	1.24	0.05	0.03
SCC × 10^3 cells/mL	19.6	26.9	7.0	0.40

[1]Statistically significant differences between treatments were determined with a threshold *P*-value <0.05. The evaluation of all independent responses considered the fixed effect of treatment, cohort, and treatment × cohort interaction. Cow nested within treatment was considered as the random effect. A detailed report of these variables over the entire experimental period is available in Ellet et al. (2024).

Table 2. Corresponding secondary antibodies used were mouse anti-rabbit IgG-HRP (catalog no. sc-2357, Santa Cruz Biotechnology) and goat anti-mouse IgG_1-HRP (catalog no. sc-2060, Santa Cruz Biotechnology).

RNA-to-DNA Ratio

Genomic DNA and total RNA quantities were determined using the AllPrep DNA/RNA Mini Kit (QIAGEN). Briefly, frozen tissue samples were weighed to ensure no more than 30 mg were used and homogenized by hand using a 5-mL glass tissue grinder. The homogenized lysate was centrifuged using individual spin columns at 8,000 × *g* for 30 s at 4°C. Flow-through was used to purify total RNA, and nucleic acids bound to the silica membrane were used to purify genomic DNA following the manufacturer's protocol. Purified RNA and DNA concentration were determined using a Nano-Drop 1000 spectrophotometer (Thermo Fisher Scientific Inc., Wilmington, DE). Total RNA and DNA were calculated by multiplying RNA or DNA concentration by the total volume. The RNA-to-DNA ratio was calculated by dividing total RNA by total genomic DNA; this is an acknowledged measurement of metabolic activity.

Statistical Analysis

All statistical analyses were performed using SAS (version 9.4, SAS Institute Inc., Cary, NC). Descriptive statistics were obtained using the UNIVARIATE procedure to test normality using the Shapiro-Wilk test. The proportion of living and dead epithelial and immune cells present in milk and not following a normal distribution was log or Box-Cox transformed to fulfill the normality assumption. All statistical analysis was performed using the GLIMMIX procedure of SAS. The evaluation of all independent responses considered the fixed effect of treatment, cohort, and treatment by cohort interaction. Cow nested within treatment was considered as the random effect. For cell loss analyses, period one was used as baseline and included as covariate in the model. Model selection was completed using a backward selection method, where no statistically significant predictor variables were removed and the model with the best fit, based on Akaike information criteria, was used. Significance was established at $P \leq 0.05$, and trends were established at $P \leq 0.10$. Data are expressed as LSM ± SEM. Milk cell data are presented as $\log_{10}$ or Box-Cox transformed LSM with 95% CI.

RESULTS

The values for respiration rate, rectal temperature, MY, and yield of milk components at the end of treatment are presented in Table 3. The complete dataset for these parameters can be found in Ellett et al. (2024). Respiration rates and rectal temperatures were increased for cows during HS, which was indicative of treatment effectiveness ($P \leq 0.01$). Cows exposed to a 4-d period of HS produced 4.3 less kg milk on the last day compared with PFTN cows ($P = 0.01$). Fat yield and protein yield decreased for HS cows by 13% and 17%, respectively ($P \leq 0.05$).

To determine whether HS directly influences cell shedding from the bovine mammary gland, flow cytometry and cell surface markers were used to evaluate cell losses of MEC and hematopoietic cells present in milk. The combined labeling of the 3 cell surface markers used in this study (butyrophilin [**BTN**] 1A1, CD45, and CD14) resulted in the identification of 8 different subpopulations. Cells in milk were assessed on a yield and concentration basis with similar results. The data were transformed to achieve a normal distribution for analysis and results are presented as $\log_{10}$ and Box-Cox LSM calculated from a yield basis (Table 4). There were no changes observed in live or dead MEC ($BTN^+CD45^-CD14^-$), macrophages ($BTN^-CD45^+CD14^+$), or hematopoietic ($BTN^-CD45^+CD14^-$) cells in milk between treatments. Live and dead putative progenitor cells ($BTN^-CD45^-CD14^+$) present in milk increased in cows under HS conditions

by 3.3 times and 3.9 times compared with PFTN cows, respectively (estimates based on back-transformed data; $P \leq 0.02$). Live triple-negative cells, with an unknown identity, tended to increase 2-fold in cows under cyclical HS compared with PFTN cows (estimates based on back-transformed data; $P = 0.08$). Conversely, yield of dead triple-negative cells decreased slightly in milk samples from HS cows (estimates based on back-transformed data; $P = 0.04$). Dead $BTN^{+}CD45^{+}CD14^{-}$ cells, with an unknown identity in milk, tended to decrease by 43% under HS conditions (estimates based on back-transformed data; $P = 0.06$).

To evaluate key changes occurring in the mammary epithelium due to the direct effect of HS, bovine mammary gland tissue was evaluated histologically. Perceptible differences were observed in the microstructure of the mammary gland after 4 d of cyclical HS (Figure 1A and 1B). The quantitative evaluation revealed that alveolar area, presented in Figure 1C, was reduced by 25% (PFTN: 10,953 vs. HS: 8,175 μm^2; $P = 0.002$) in cows exposed to HS. In agreement with this, alveoli number per area was greater in tissue from HS cows compared with PFTN cows (Figure 1D; PFTN: 22.3 vs. HS: 26.4 alveoli; $P = 0.03$). The total nucleated MEC per area was 21% greater in mammary gland tissue samples from cows under HS conditions (Figure 1E; PFTN: 321 vs. HS: 389 cells; $P = 0.01$). However, the number of nucleated MEC per individual alveolus did not differ between treatments (Figure 1F; PFTN: 26.3 vs. HS: 24.9). Additionally, the correlation coefficient between alveolar area and MY was evaluated and found to be weak ($r < 0.25$) and nonsignificant.

Transcript expression of previously reported genes involved in nutrient transport, *GLUT1* and *GLUT8* (glucose transporters 1 and 8); milk component synthesis, *CSN2* (β-casein), *CSN3* (κ-casein), *LALBA* (α-lactalbumin), and *FASN* (fatty acid synthase); and heat response, *HSP70*, *HSPA5*, and *HSPA8* (heat shock protein family A, A5, and A8), were evaluated (Figure 2). There were no treatment differences in the relative fold expression for any of the evaluated transcripts. To further evaluate cell activity, the relative abundance of proteins involved in cell survival, cell differentiation, and protein synthesis was assessed by immunoblotting (Figure 3). From targets involved in the Janus kinase/signal transducers and activators of transcription (**JAK/STAT**) signaling pathway (Figure 3A), phosphorylated STAT 5 (**pSTAT5**) abundance decreased in mammary gland tissue samples from cows exposed to HS compared with PFTN cows. Total STAT5 and prolactin receptor abundance were not affected by treatment. Within the mitogen-activated protein kinase (**MAPK**) signaling cascade (Figure 3B), a tendency to decrease the extracellular signal-regulated kinase 1 and 2 (**ERK**) abundance and to increase the MAPK abundance was observed in mammary gland tissue samples from HS cows. For the mammalian target of rapamycin (**mTOR**) pathway (Figure 3C and D), phosphorylated protein kinase B (**pAKT**), AKT, ribosomal protein S6 kinase β-1 (S6K1), and the eukaryotic translation initiation factor 4E binding protein 1 (4EBP1) protein abundance did not differ between treatments. However, phosphorylated S6K1 abundance decreased in tissue samples from HS cows. For the proteins involved in autophagy (Figure 3E), the lipidated microtubule-associated protein light chain 3 (LC3 II) abundance increased considerably in tissue samples from HS cows compared with PFTN cows. However, autophagy-related protein 7 (ATG7) abundance did not change between treatments. The ratio of phosphorylated and total proteins is presented in Figure 4 and there were no significant differences for any of the proteins evaluated.

Finally, as a companion measurement for metabolic activity, the RNA-to-DNA ratio was evaluated on mammary tissue homogenates and did not differ between HS and PFTN cows (Figure 5; PFTN: 1.46 vs. HS: 1.32).

DISCUSSION

Physiological responses such as increased respiration rate and rectal temperature are main criteria for determining thermal stress in dairy cows (do Amaral et al., 2011; Tao et al., 2012; Fabris et al., 2017). Respiration rate and rectal temperature observed in HS cows suggest inadequate evaporative heat dissipation from the skin surface. The increase in both parameters supports the effectiveness of temperature regulation and HS treatment in this study. Additionally, the pair-feeding model mitigated the reduced DMI effects between treatments induced by HS, revealing the direct effects of HS on the mammary gland microstructure, cell activity, and cell loss.

Milk yield reductions due to HS are the most tangible and widely reported effects directly associated with revenue losses on a dairy farm. As expected, MY decreased 4.3 kg on the fourth and last day of treatment for cows under cyclical HS compared with PFTN cows. This result is similar to previous studies that reported around 7.5 kg/d less milk in midlactation multiparous Holstein cows exposed to HS (THI from 73 to 82) for 9 d compared with pair-fed thermoneutral cows (THI = 64; Rhoads et al., 2009). The increased loss in milk compared with the present investigation might have occurred due to the extended HS period. However, it has been reported that the highest effect of HS on MY occurs after 4 d under noncontrolled conditions (Spiers et al., 2004; Bernabucci et al., 2014). Protein and fat yield reduction were mainly driven by the reduction in MY. There were no differences in milk protein and fat concentrations between treatments (data not shown), which agreed with previous studies

Table 4. Log_{10} and Box-Cox LSM (95% CI) calculated for cell yield of each milk cell subpopulation from the morning milking; data were obtained from cows exposed to controlled thermoneutral (THI of 64; n = 8) or cyclical HS (THI from 74 to 80; n = 7) conditions over a 4-day period

				PFTN			HS			
					95% CI			95% CI		
Status[1]	Cell labeling[2]	Identity	Transformation[3]	LSM[4]	Lower	Upper	LSM[4]	Lower	Upper	*P*-value[5]
Live	$BTN^-CD45^-CD14^-$	Unknown	Log_{10}	1.15	−0.38	2.67	1.49	−0.16	3.15	0.08
	$BTN^-CD45^+CD14^-$	Hematopoietic	Box-Cox	3.07	2.67	3.46	3.06	2.63	3.49	0.90
	$BTN^-CD45^+CD14^+$	Macrophages	Box-Cox	2.79	2.40	3.17	2.80	2.38	3.22	0.76
	$BTN^-CD45^-CD14^+$	Potential progenitors	Log_{10}	1.04	0.78	1.30	1.56	1.28	1.84	0.02
	$BTN^+CD45^-CD14^-$	MEC	Log_{10}	0.01	−0.22	0.25	−0.22	−0.47	0.02	0.17
	$BTN^+CD45^+CD14^-$	Unknown	Log_{10}	0.31	−0.15	0.77	0.10	−0.40	0.60	0.51
	$BTN^+CD45^+CD14^+$	Unknown	Log_{10}	0.48	−1.02	1.98	0.37	−1.26	2.00	0.54
	$BTN^+CD45^-CD14^+$	Unknown	Log_{10}	0.61	−0.89	2.12	0.36	−0.93	1.66	0.19
Dead	$BTN^-CD45^-CD14^-$	Unknown	Box-Cox	1.39	1.32	1.47	1.37	1.29	1.45	0.04
	$BTN^-CD45^+CD14^-$	Hematopoietic	Box-Cox	2.41	2.38	2.44	2.42	2.39	2.44	0.64
	$BTN^-CD45^+CD14^+$	Macrophages	Box-Cox	2.76	2.57	2.95	2.75	2.55	2.95	0.65
	$BTN^-CD45^-CD14^+$	Potential progenitors	Log_{10}	1.50	−0.15	3.15	2.09	0.30	3.87	0.01
	$BTN^+CD45^-CD14^-$	MEC	Log_{10}	0.54	−1.00	2.09	0.52	−1.08	2.12	0.90
	$BTN^+CD45^+CD14^-$	Unknown	Log_{10}	0.10	−0.92	1.11	−0.15	−1.24	0.94	0.06
	$BTN^+CD45^+CD14^+$	Unknown	Box-Cox	−0.19	−0.77	0.39	−0.53	−1.16	0.10	0.41
	$BTN^+CD45^-CD14^+$	Unknown	Log_{10}	0.92	0.13	1.71	0.85	0.06	1.63	0.42

[1]Cell viability was assessed using PI (BD Biosciences, 5 µg/mL).

[2]Cells were labeled for cell surface proteins for hematopoietic cells (CD45; clone CACTB51A, Kingfisher Biotech, 3.1 ng/µL), macrophages (CD14; clone CAM 36A, Kingfisher Biotech, 1.25 ng/µL), and MEC (BTN 1A1; clone 2151C conjugated to APC, NOVUS Biologicals, 7 ng/µL).

[3]Lambda values: $BTN^-CD45^-CD14^-$ (dead: $\lambda = -0.75$), $BTN^-CD45^+CD14^-$ (live: $\lambda = -0.35$; dead: $\lambda = -0.45$), $BTN^-CD45^+CD14^+$ (live and dead: $\lambda = -0.40$), $BTN^+CD45^+CD14^+$ (dead: $\lambda = 0.45$).

[4]Original untransformed data were expressed as 10^3 cells per milking and transformed using log_{10} and Box-Cox transformation for statistical analysis.

[5]Significant differences between treatments were determined with a threshold *P*-value <0.05. The evaluation of all independent responses considered the fixed effect of treatment, cohort, and treatment × cohort interaction. Cow nested within treatment was considered as the random effect. Data from period 1 was used as baseline and included as a covariate in the model.

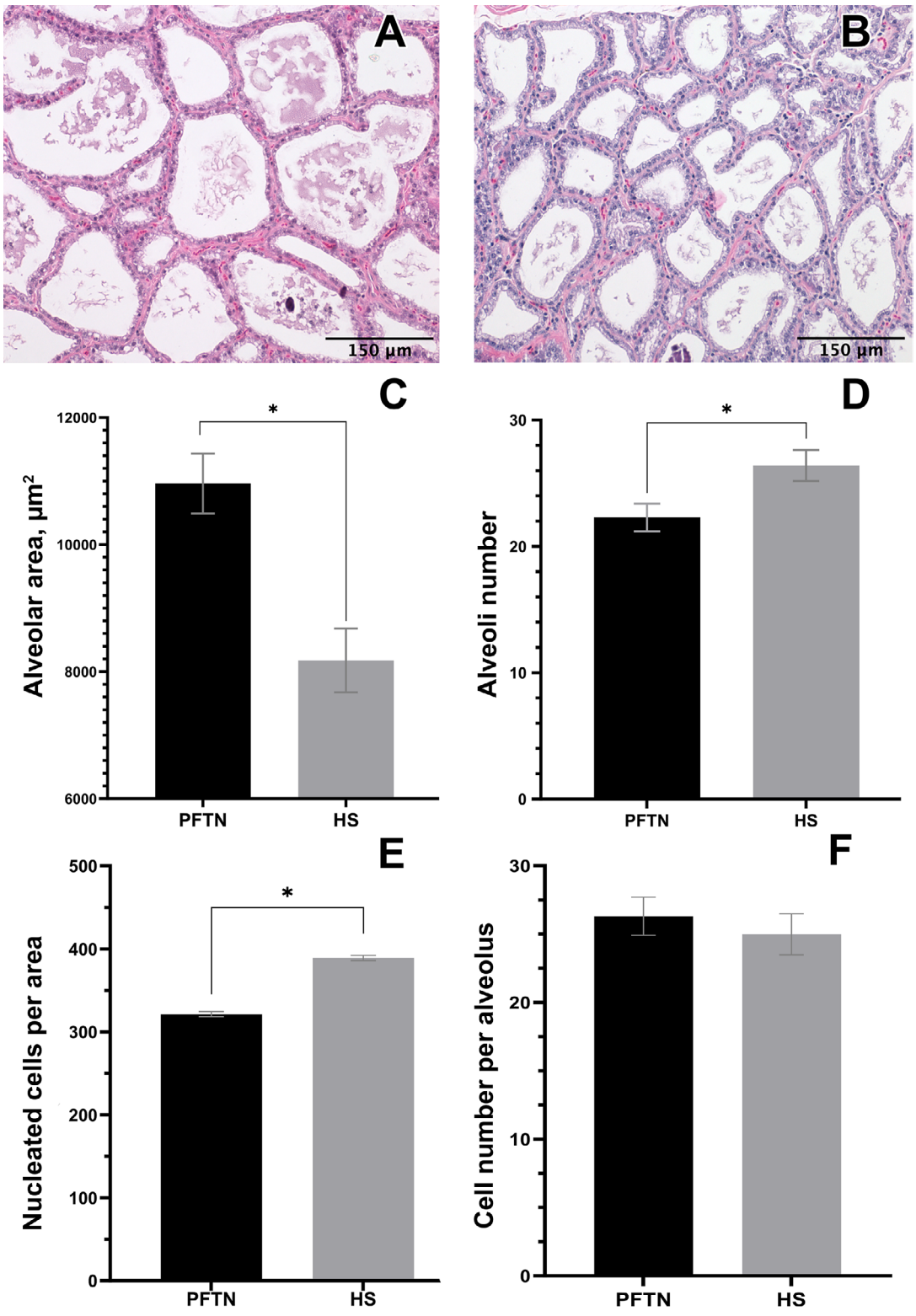

Figure 1. Histology analysis of the lactating mammary gland from multiparous Holstein cows exposed to PFTN (THI = 64; n = 8) or HS conditions (THI = 74–80; n = 7) for 4 d. Panels A and B show representative images for H&E stained mammary tissue at 20× original magnification exposed to PFTN (A) or HS (B) conditions. Alveolar area (C) and alveoli number (D) in mammary gland samples from lactating Holstein cows exposed to PFTN (black bars; n = 8) or HS (gray bars; n = 7) conditions for 4 d. Nucleated mammary epithelial cells per an area of 304,821 µm^2 (E) and cell number per alveolus (F) in mammary gland samples from lactating Holstein cows exposed to PFTN (black bars; n = 8) or HS (gray bars; n = 7) conditions for 4 d. Data presented are LSM ± SEM. An asterisk (*) indicates a statistically significant difference between treatments (P-value < 0.05).

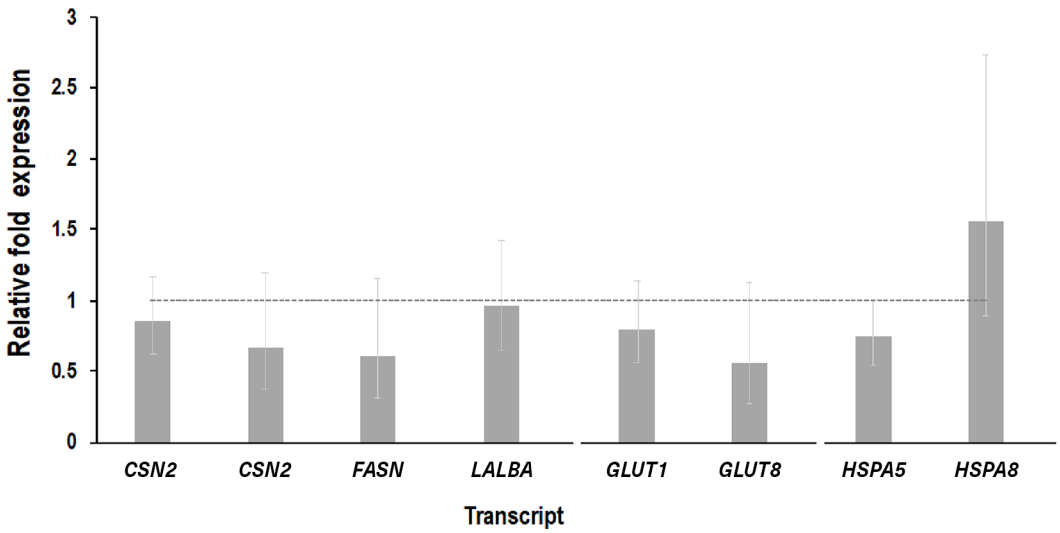

Figure 2. Gene expression in mammary gland tissue samples from lactating Holstein cows exposed to PFTN (THI = 64; n = 8) or HS (THI = 74–80; n = 7) conditions for 4 d. Gene expression is reported as fold expression ($2^{-\Delta\Delta CT}$) relative to pair-fed cows and under thermoneutral conditions. Error bars denote 95% CI. The reference expression level of PFTN cows is represented by the dotted line. No significant differences in gene expression were observed between the treatment groups.

reporting no differences for fat (Smith et al., 2013) and protein (Hammami et al., 2015; Weng et al., 2018) concentration in milk from cows exposed to HS conditions.

Based on MY reduction observed in this study, we hypothesized that a short period of HS might trigger a reduction in the chief factors controlling milk synthetic capacity of the secretory epithelium (i.e., measures of MEC number and activity) of the bovine mammary gland. We propose that these are potential mechanisms, independent of DMI reduction, for the rapid decrease in MY observed under HS during lactation in high-producing Holstein cows. To investigate the effects of HS on both cell number and cell activity, we evaluated a range of variables related to these cell features. Mammary epithelial cell number was evaluated for losses into milk and histologically in mammary gland tissue, and cell activity was evaluated by gene transcription and protein abundance measures in mammary gland tissue samples.

Quantity and metabolic activity of secretory MEC determine the mammary gland milk synthesis capacity (Stefanon et al., 2002; Akers, 2016). The number of secretory MEC in the gland fluctuates across lactation and is determined by proliferation and cell death rate (Capuco et al., 2001). Most literature describes changes in MEC death by apoptosis. However, other mechanisms of cell loss occur in the mammary gland, including MEC exfoliation during lactation. Herve et al. (2016) propose that MEC exfoliation can play a partial role in controlling cell number in the mammary gland. Mammary epithelial cell exfoliation can be modified by factors such as lactation stage (Boutinaud et al., 2013), endocrine status (Lollivier et al., 2015), management (Ben Chedly et al., 2013), and environmental factors (Lengi et al., 2022). We evaluated MEC loss into milk, our measure of MEC exfoliation, to examine this mechanism of potential reductions in cell number based on the assumption that MEC present in milk, identified by BTN, the major protein of bovine milk fat globule secretion, were functional secretory cells in the gland. It has been shown that most of the exfoliated epithelial cells present in milk are viable and exhibit characteristics of fully differentiated alveolar cells (Boutinaud and Jammes, 2002). Live and dead BTN^+ cells in milk were not affected by treatment in this study. These results are divergent from a previous study that reported an 82% and 78% increase in total and live BTN^+ cells, respectively, in milk from cows exposed to HS for 9 d (Lengi et al., 2022). Although the methods used in our study and the referred study were the same, other factors might explain differences. Lengi et al. (2022) evaluated the effects of HS without using a pair-feeding model, and it is possible that the effects on BTN^+ cell loss are mainly an effect of DMI reduction and impaired nutrient availability for the mammary gland and the MEC, leading to a lack of support for secretory MEC maintenance. This has been demonstrated in previous studies, where animals in thermoneutral conditions that were feed-restricted by 20% of ad libitum DMI had a 65% greater daily MEC exfoliation rate in milk (Herve et al., 2019). Another crucial factor that differentiates our study and the study by Lengi et al. (2022) is the exposure time of HS, which was greater by 2.25-fold (4 vs. 9 d). Heat stress exposure duration might play a significant role in the response of

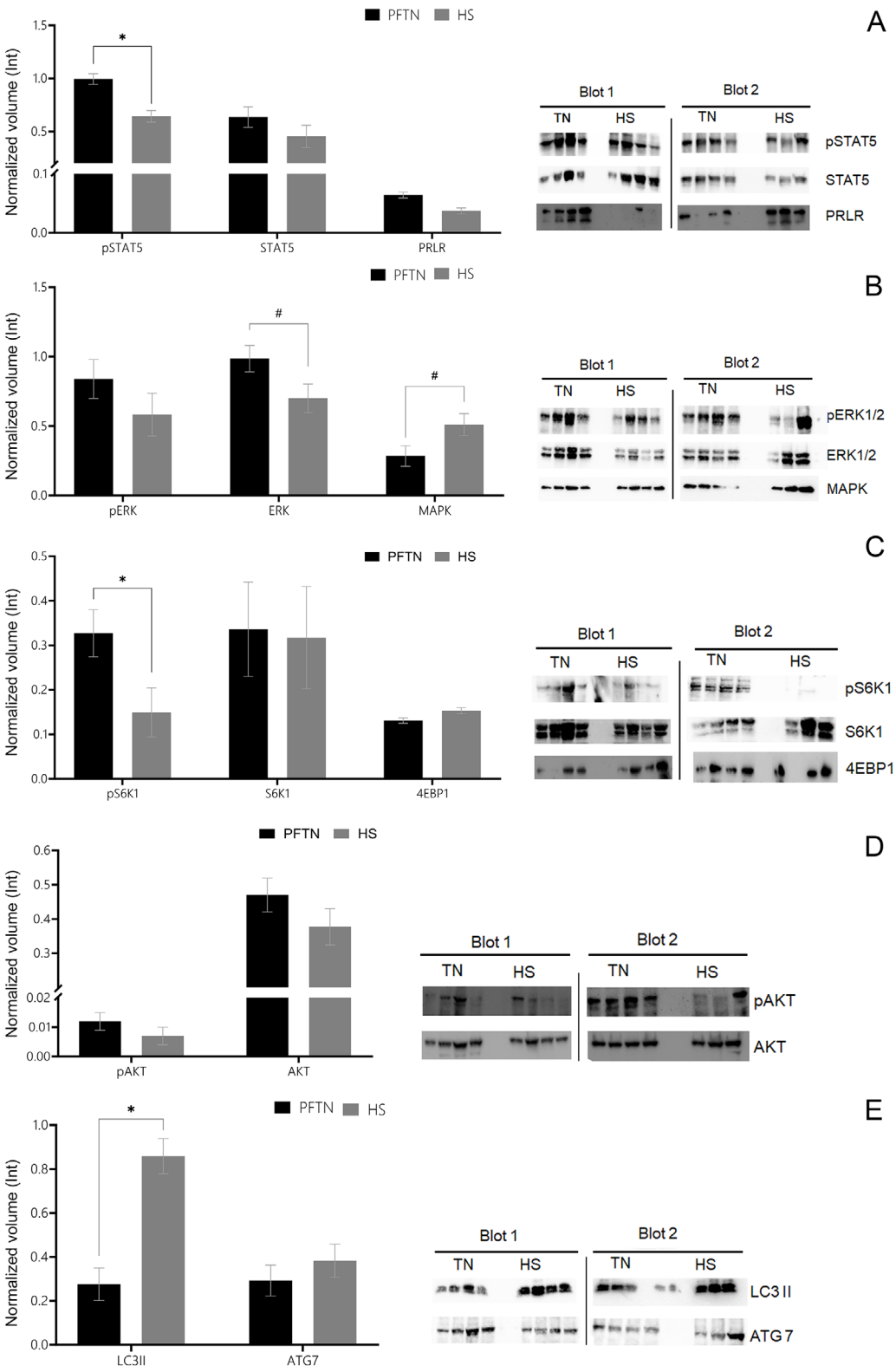

Figure 3. Protein relative abundance (Int = intensity) from targets involved in the JAK/STAT signaling pathway (A), MAPK signaling cascade (B), mTOR pathway (C and D), and autophagy (E) in mammary gland tissue samples from lactating Holstein cows exposed to PFTN (THI = 64; black bars; n = 8) or HS (THI = 74–80; gray bars; n = 7) conditions for 4 d. Data presented are LSM ± SEM. An asterisk (*) indicates a significant difference (P-value <0.05) and a pound sign (#) indicates a tendency (0.05 < P-value ≤ 0.15) between treatments. The Western blot analysis comprised 15 samples from both treatment groups distributed in 2 blots (blot 1, n = 7; and blot 2, n = 8).

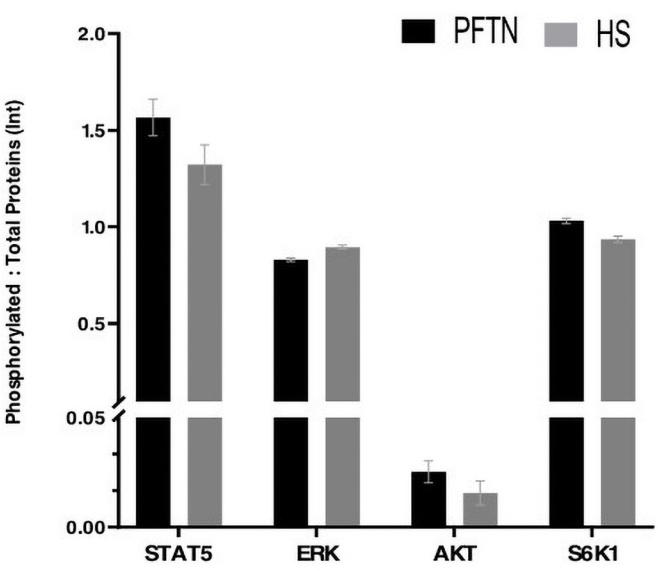

Figure 4. Ratio of phosphorylated protein to total protein (Int = intensity) in mammary gland tissue samples from lactating Holstein cows exposed to PFTN (THI = 64; black bars; n = 8) or HS (THI = 74–80; gray bars; n = 7) conditions for 4 d. Data presented are LSM ± SEM. No significant differences were observed between the experimental groups.

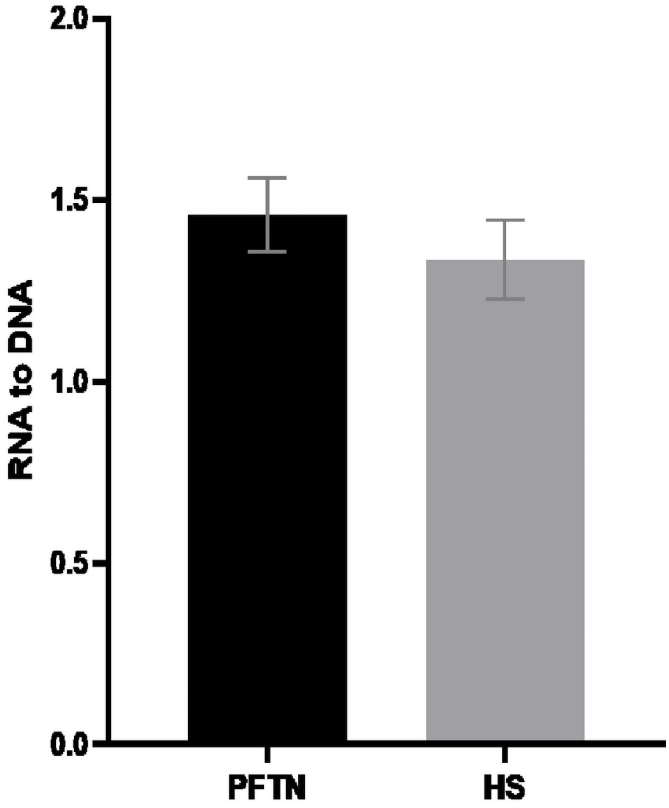

Figure 5. RNA-to-DNA abundance in mammary gland tissue samples from lactating Holstein cows exposed to PFTN (THI = 64; black bars; n = 8) or HS (THI = 74–80; gray bars; n = 7) conditions for 4 d. Data presented are LSM ± SEM. No significant differences were observed between the experimental groups.

the mammary gland and the pattern of cell shedding. The results observed in this study suggest that cows exposed to HS longer might produce a chronic response in the secretory MEC that cannot be achieved under 4 d of cyclical HS. Additionally, Lengi et al. (2022) compared BTN^+ cells in milk from the same cow, in contrast to our study where we compared cells from different cows. We observed substantial variability across samples from animals in different treatments, making it challenging to detect significant differences between treatments. However, due to our experimental design involving slaughter for sample collection, repeated sampling of the same cows on different treatments was not possible.

To further analyze cell number using a direct approach, we evaluated secretory MEC number through histology analysis. Cell number per alveolus was not affected by HS, aligning with the lack of HS effect on the exfoliation yield of MEC in milk. There are no reports in the literature evaluating the effects of HS during lactation on bovine MEC number. However, in vitro studies using isolated MEC from mouse mammary gland have demonstrated that MEC number is reduced by 55% when cultured at 41°C for 2 d compared with 37°C (Wakasa et al., 2022). The lack of differences in MEC number in this study might be explained by the moderate HS conditions used, as indicated by the comparatively low differences in rectal temperature among cows exposed to PFTN and HS conditions (1.4°C), whereas the in vitro work had a wider range of 4°C between treatments (Wakasa et al., 2022). Combined with this, the average rectal temperature reached in HS cows was 40°C. West et al. (2003) proposed that an increase in ambient temperature will increase mammary gland inner temperature indirectly. Nevertheless, an increase greater than 41°C for a substantial period occurring in the gland seems unlikely. Although cell number per alveolus was not affected, cell number per area was greater in tissue samples from HS cows compared with PFTN cows. This was mainly caused by the evident structural changes in the mammary gland secretory tissue. Individual alveolus area was reduced by 25% and, consequently, alveoli number per area increased by 18% in tissue samples from cows exposed to cyclical HS for 4 d. The possibility that the differences observed in alveolus area and alveoli number occurred due to differences in final milking and slaughtering time between HS and PFTN cows was considered. However, this was unlikely given similar milking-to-slaughtering interval (PFTN, 3.35 ± 1.2 h vs. HS, 3.07 ± 0.8 h).

Mammary gland tissue samples from cows exposed to intrauterine HS during fetal development showed a 46% reduction in alveoli area during their first lactation com-

pared with samples from animals maintained in cooled conditions during fetal development (Skibiel et al., 2018). However, contrary to what we observed, in Skibiel et al. (2018) alveoli number did not differ between treatments. Dado-Senn et al. (2019) observed a 15% decrease in alveoli number in mammary gland samples obtained during lactation from multiparous cows exposed to HS during the entire dry period immediately preceding lactation. The lack of consistent results of the effect of HS on bovine gland structure from these studies might be explained by the differences between HS time exposure (4 d vs. 46 d), exposure occurring at different developmental stages (fetal vs. mature), physiological state (lactation vs. dry period), or a combination of these factors. Heat stress might influence the mammary gland differently during the dry period versus lactation. The dry period is a nonlactating phase between lactations where senescent MEC differentiate into terminally differentiated, more metabolically active cells for the next lactation, and HS might directly affect MEC number (proliferation vs. cell death) during this period (Dado-Senn et al., 2018). In contrast, it is known that HS can affect intracellular signaling pathways responsible for productivity (Collier et al., 2008). During established lactation, in the mammary gland a remarkable and dynamic process occurs, leading to changes in the size of individual alveoli, the functional units responsible for milk production. Still, the specific cellular mechanisms responsible for the area decrease in individual alveoli during lactation remain largely unknown and represent an area of active research and scientific inquiry. However, the sole reduction of the MEC capacity to synthesize milk could decrease luminal area, and thus drive individual alveolus area reduction observed in mammary gland tissue samples obtained from cows under HS.

To evaluate the synthetic capacity or cell activity of the bovine mammary gland, we measured the transcript abundance of genes related to signaling pathways involved in cell activity, heat response, solute transport, and the expression of proteins involved with cell survival, cell differentiation, and protein synthesis. Protein and fat encoding gene expression were not affected by treatment (*CSN2*, *CSN3*, *LALBA*, and *FASN*). This agrees with the results of Cowley et al. (2015) who reported no differences for β- and κ-casein in milk samples from midlactation Holstein cows exposed to HS for 7 d compared with milk samples from ad libitum and pair-fed thermoneutral cows. On the other hand, it has been observed that HS decreased *CSN2* and *CSN3* gene expression in mammary gland tissue from lactating Holstein cows exposed to a noncontrolled ambient HS for 21 d (Yue et al., 2020). Similarly, in a controlled crossover study using lactating multiparous cows exposed to HS during 9 d, the expression of milk protein-encoding genes (*CSN3* and *LALBA*) in mammary gland tissue samples was downregulated compared with samples from the PFTN group (Gao et al., 2019). Fatty acid synthase (*FASN*), unaffected by HS in our study, is the major enzyme involved in fatty acid synthesis in the ruminant mammary gland (Smith, 1994). In vitro studies have shown a decrease in protein expression of *FASN* in cultured MEC exposed to HS for 1 h at 40°C (Li et al., 2017).

Multiple nutrients are essential for milk synthesis, including glucose, which is taken up by MEC through specific transporters. Here we evaluated the transcript expression of glucose transporters 1 and 8. Gene expression levels were unaffected by HS. Glucose transport in the lactating mammary gland is essential for multiple processes such as lactose synthesis, *NADPH* generation, milk lipid synthesis, energy production, and nucleic acid and amino acid synthesis (Zhao, 2014). In the bovine mammary gland, the expression of *GLUT1* and *GLUT8* has been reported (Zhao et al., 2004). Particularly, in bovine mammary gland biopsies obtained from lactating cows exposed to HS for 9 d, a decrease in *GLUT1* and *GLUT8* gene expression was observed compared with tissue samples from pair-fed thermoneutral cows (Gao et al., 2019).

To evaluate the effect of HS on heat shock response in mammary tissue, we evaluated gene expression of 2 orthologs of the HSP70 family, *HSPA5* and *HSPA8*. Heat shock proteins are highly conserved and their production is characterized as a cellular response to HS (Tao et al., 2018). The HSP70 family protects the cell from detrimental HS effects by functioning as a chaperone and stabilizing proteins in a folding-competent state. Contrary to what was observed in previous in vitro studies, neither of the 2 HSP70-related genes evaluated was affected by HS. It has been shown that HSP70 gene and protein expression was upregulated in 2 different in vitro studies where MEC were incubated at 42°C for more than 30 min (Collier et al., 2008; Hu et al., 2016).

The absence of discernible differential gene expression observed in our study might have occurred due to the sample type used. The use of mammary tissue homogenates in our study introduces an inherent complexity to the analysis of gene expression. Although cell culture experiments can provide valuable insights into specific cellular behaviors, studying gene expression in whole tissue homogenates allows us to capture the collective response of various cell types within the mammary gland. However, the heterogeneity of mammary tissue homogenates presents both opportunities and challenges in interpreting the differential gene expression results. The complexity of the tissue allows us to investigate the regulatory interactions between different cell types and understand how they collaborate to achieve a specific biological function, such as milk production in lactation, but the presence of

multiple cell types can introduce noise and variability to the data, potentially masking subtle gene expression changes specific to MEC.

The connection between gene expression and protein expression is crucial, because the information encoded in the gene's DNA sequence determines the sequence of amino acids in the resulting protein. However, it is essential to recognize that not all transcribed genes will be translated into proteins or that translation will be proportional to transcription. In general terms, the lack of significant changes in gene expression of the targets evaluated here might be explained by the shorter period of HS exposure compared with the aforementioned studies and temperatures used in the in vitro studies. Gene transcription changes produced by environmental alterations allow for a physiological adaptive response (Feugeas et al., 2016); however, the evaluation of gene expression only reflects the steady-state abundance of mRNA, a function determined by mRNA production and turnover rate (Schwanhäusser et al., 2011). Based on this, the evaluation of transcript translation and protein synthesis could show different results because proteins are the main regulators of cell function. Heat stress affects numerous intracellular signaling pathways responsible for cell maintenance, productivity, and survival (Collier et al., 2008). To further evaluate these effects, proteins involved in cell survival, cell differentiation, and protein synthesis pathways were evaluated by immunoblotting. Among all target proteins evaluated, only pSTAT5 and pS6K1 decreased and LC3 II increased significantly in the tissue samples from HS cows.

The JAK/STAT pathway is crucial in the regulation of milk and milk protein synthesis in the mammary gland. This pathway is activated by prolactin signaling that works in conjunction with other lactogenic hormones to induce cell differentiation and promote the expression of mRNA encoding milk proteins. One of the key components involved in this process is the transcription factor STAT5. Through its activation by prolactin, STAT5 plays a significant role in regulating the genes responsible for milk protein synthesis (Watson and Burdon, 1996).

In vitro studies have shown that a 3 d exposure of cultured MEC to HS at 41°C leads to the inactivation of STAT5 and a decrease in milk synthesis capacity (Kobayashi et al., 2018). In vivo studies have demonstrated a decrease in gene and protein expression of prolactin receptor (**PRLR**), STAT5A, STAT5B, and JAK2 in bovine mammary gland tissue homogenates from cows exposed to 3 wk of environmental HS (THI from 72.5 to 86.9; Yue et al., 2020). In the present investigation, only pSTAT5 was significantly reduced in HS and no effects of HS were observed for STAT5 and PRLR. This might indicate that a short period of HS does not alter the synthesis of STAT5, but its activation instead. A reduction of pSTAT5, an important regulator of milk synthesis, suggests a decrease in the synthetic capacity of the bovine secretory MEC under HS.

The MAPK intracellular signaling cascade with the ERK1/2 pathway is implicated in MEC function (Krishna and Narang, 2008). In this study, a tendency for increased and decreased protein abundance of MAPK and ERK1/2 was observed, respectively, under HS conditions. There are no reports available in the literature evaluating the effects of HS on the MAPK signaling cascade and its effectors in the bovine mammary gland. Despite this, Kyoto Encyclopedia of Genes and Genomes analysis on mammary gland tissue samples from cows exposed to environmental HS for a month showed an enrichment effect of 72 differentially expressed microRNAs involved in the MAPK pathway, suggesting that HS may influence the MAPK pathway to reduce mammary gland function (Fan et al., 2021). The observed rising trend in MAPK protein abundance in this study, an essential regulator of the immune response, suggests the amplification of cellular responses to guarantee cell survival and promote inflammatory responses. Additionally, one of the most recognized biological functions of ERK1/2 is cell proliferation, differentiation, and survival (Pearson et al., 2001). Although there are no reports evaluating ERK1/2 in the bovine mammary gland under HS conditions, the relative expression of phosphorylated and total ERK1/2 increased in murine mammary organoids cultured at 41°C for 3 d compared with mammary organoids cultured at 37°C (Wakasa et al., 2022). What was reported in this study does not align with what was observed in our study, where total ERK1/2 protein abundance tended to decrease in mammary tissue samples obtained from cows exposed to HS for 4 d. The downregulation of ERK1/2 in the bovine mammary gland under acute HS might indicate a reduction in cell proliferation and differentiation, suggesting a prioritization of resources toward survival mechanisms rather than growth processes.

This downregulation might signify a redirection of cellular energy toward thermoregulatory functions instead of MEC turnover. Prior studies using in vitro models have shown that HS can inhibit cell proliferation in bovine MEC. Bovine MEC subjected to incubation at 42°C for 12 h reduced the relative expression of miR-425–5p levels, a pivotal regulator of cellular proliferation. Furthermore, both relative gene expression and protein abundance of *PCNA* and *MCM3*, essential regulators of DNA replication and repair, exhibited significant decreases under these conditions (Li et al., 2024).

Another protein involved in cell survival and growth is mTOR. This kinase is predominantly activated by the PI3K/AKT pathway, where AKT directly phosphorylates and activates mTOR. Other proteins involved in this pathway are 4EBP1, a translation inhibitor, and S6K1,

a protein kinase, which participate in protein synthesis (Berchtold and Walther, 2009; Kakumoto et al., 2015). Of the PI3K/AKT/mTOR proteins evaluated in this study, only phosphorylated S6K1 (**pS6K1**) protein abundance was reduced in mammary gland samples from HS cows. In agreement with what was observed in our study, previous studies found that pS6K1 protein abundance decreased at 42 and 84 d of lactation in mammary gland samples from cows exposed to HS during the entire dry period (~46 d) compared with cooled cows (Dado-Senn et al., 2021). Furthermore, in the same study, converse to what we observed in this study, a decrease in protein abundance for AKT at 84 d of the lactation was observed. Agreeing with our results, no changes for 4EBP1 protein abundance were observed in mammary gland samples from cows exposed to environmental HS during the dry period (Dado-Senn et al., 2021). The differences observed between these studies might originate from the time exposure to HS difference (46 vs. 4 d) and the physiological state (dry period vs. lactation) when HS was imposed.

Of the 2 autophagy-related proteins evaluated in this study, only LC3 II protein relative abundance increased considerably with no changes observed in ATG7 in mammary gland samples from lactating cows exposed to cyclical HS for 4 d. Mammary epithelial cell death in the mammary gland occurs across lactation and can be altered by HS. In vitro studies have shown that programmed cell death increases at 42°C in incubated mammary tissue explants of HS cows and bovine MEC (Cai et al., 2018; Chen et al., 2020; Ouellet et al., 2021). Programmed cell death includes 3 major cell death types: apoptosis, autophagy, and necrosis (Andón and Fadeel, 2013). The most described programmed cell death type in the bovine mammary gland is apoptosis. Nevertheless, it has been shown that autophagy plays a crucial role during the dry period to support postlactation bovine mammary gland regression (Motyl et al., 2007). Multiple papers have shown an alteration in autophagy-related proteins and transcripts during the dry period after HS (as reviewed by Tao et al., 2018). However, the incidence of autophagy in bovine mammary gland tissue exposed to HS during lactation has not been described. The increase in LC3 II abundance, a protein that participates in engulfment and autophagosome formation, at d 14 relative to dry off increased in mammary gland tissue samples from cows exposed to HS during the dry period (Wohlgemuth et al., 2016). In agreement with the results observed in this study, previous reports have not observed changes in ATG 3, 5, and 7 at transcript and protein levels in mammary gland samples from cows exposed to HS during the dry period (Wohlgemuth et al., 2016; Ouellet et al., 2021). The increased level of LC3 II shows that autophagy and phagosome formation is activated after a short period of HS, suggesting an increase in damaged cell organelles that could decrease the synthetic capacity of MEC under HS. Furthermore, the lack of changes in MEC number in milk and tissue suggests that autophagy might be activated to remove dysfunctional cell components, to guarantee cell survival instead of cell death during short periods of HS.

Finally, to evaluate the overall synthetic capacity in the mammary gland tissue we evaluated the ratio between RNA and DNA. Most of the RNA measured in the sample is rRNA, reflecting the amount of protein synthesis occurring at the individual cell level, whereas the DNA measured amount is a fixed value per cell. Therefore, higher ratios of RNA to DNA indicate a higher synthetic capacity in the cell. The RNA-to-DNA ratio estimates in this study were not different between the treatments.

The lack of differences in RNA-to-DNA ratio between treatments in this study might be explained by a different response to acute and chronic HS. Exposure to HS for 4 d might not reveal the changes to rRNA, which could maintain a steady state during an acute response to HS. However, it is plausible that at the end of HS exposure in this experiment, RNA cellular degradation or reduced synthesis have just started. This premise agrees with what was observed with the LC3 II abundance in this study, where LC3 II abundance—an adaptor protein involved in intracellular degradation—increased significantly in the HS cows, suggesting an increase in phagosome degradation of cell organelles and components. It seems probable that after an extended time of HS exposure, RNA degradation or a lack of synthesis as a response to reduced milk production will occur and a difference in RNA-to-DNA ratio could be observed.

Although no quantitative changes in SCC were observed in the study, the possibility of alterations in the immune population existed. Heat stress might impair the immune function of the bovine mammary gland at the cell or organ level (Tao et al., 2018). To further explore immune cell profile in milk from bovine mammary glands under HS, we evaluated the presence of immune cells in milk using cell surface markers. In general, HS affected neither live nor dead macrophages ($CD45^+CD14^+$) consistent with previous findings assessing the effect of HS on these specific cell populations (Lengi et al., 2022). Similarly, live and dead immune cells ($CD45^+$) were not affected by HS in this study. These results contrast with the results reported by Lengi et al. (2022) where live $CD45^+$ immune cell concentration decreased 71% in milk samples from multiparous Holstein cows under HS during early lactation. The use of only 2 immune markers in the present investigation prevents us from precise cell-type identification. It is possible that because of the non-specific identities of immune cells, we might overlook changes in specific immune cell subpopulations such as

T cells or granulocytes. In vitro studies have shown impaired function in immune cell activity of mononuclear and polymorphonuclear bovine cells exposed to hyperthermia (Lacetera et al., 2006; Lecchi et al., 2016).

Additionally, alteration of other unidentified cells in milk by HS was observed including $BTN^{-}CD45^{-}CD14^{+}$, $BTN^{+}CD45^{+}CD14^{-}$, and $BTN^{-}CD45^{-}CD14^{-}$. Suggested identities for these populations are putative progenitors, unidentified dual origin cells, and other cell types not identified by the available markers used in this study. Live and dead $BTN^{-}CD45^{-}CD14^{+}$ cells increased by 300% to 400% in milk samples obtained from cows under HS for 4 d. These results agree with previous reports from our group that have shown an increase of 60% in the same cell subpopulation ($CD45^{-}CD14^{+}$) in response to HS (Lengi et al., 2022). The expression of the CD14 transcript is denoted as a progenitor cell marker in MEC from several studies in rodents and humans (Bach et al., 2017; García Solá et al., 2021; Martin Carli et al., 2021). Heat stress has adverse effects on cellular processes such as cell proliferation. It has been reported that cell proliferation is reduced during the transition period in mammary tissue samples from cows exposed to HS during the dry period (Tao et al., 2011). Heat stress might affect progenitor cells robustly within the mammary gland, directly affecting cell proliferation instead of cell death. More studies about the effects of environmental factors like HS in specific cell identities, such as progenitor cells and the presence of progenitor cells across lactation in the bovine MEC, are needed.

Live triple-negative cells, $BTN^{-}CD45^{-}CD14^{-}$, tended to increase with HS, but dead triple-negative cells decreased significantly in milk samples from HS cows. These unidentified cells can be any other differentiated or undifferentiated cell type present in milk. Potential identities for these could include myoepithelial or ductal epithelial cells because both cell types would be negative for CD45 and BTN. Nevertheless, the possibility that myoepithelial cells can be shed into milk is less likely due to their basal position inside the basement membrane. It has been reported in primary murine mammary organoids that even when luminal cells are induced to protrude into the extracellular matrix, the myoepithelial cell layer is not altered (Sirka et al., 2018). Therefore, the presence of nonsecretory epithelial ductal cells that might be exfoliated into milk is more plausible.

CONCLUSIONS

Heat stress in lactating Holstein cows contributes to a reduction in MY of 4.3 kg after 4 d of cyclical exposure. The milk yield decrease is primarily due to the impairment of pathways associated with protein synthesis and cell survival. Additionally, HS increases the autophagosome protein LC3 II, suggesting enhanced degradation of dysfunctional cell components. Our findings highlight that cell activity, rather than cell number, plays a significant role in regulating MY during the initial phase of HS. Moreover, HS exposure for 4 d results in increased shedding of live and dead $CD14^{+}$ cells, potential progenitors, into milk. These insights underscore the convoluted impact of HS on the bovine mammary gland structure and function, requiring further research to understand its effects on specific cell identities and the functionality of heterogeneous subpopulations.

NOTES

This work was supported by the USDA-NIFA Hatch Project VA-135995 (USDA, Washington, DC), Fulbright Visiting Scholar Program (to L. J. Banda; Fulbright, Washington, DC), and AFRI competitive grant no. 2020-67015-30830 (USDA, Washington, DC). The use of animals and all procedures for this investigation were approved by the Virginia Tech Institutional Animal Care and Use Committee (19-247). The authors have not stated any conflicts of interest.

Nonstandard abbreviations used: BTN = butyrophilin; CD14 = cluster of differentiation 14; CD45 = protein tyrosine phosphatase receptor type C; ERK = extracellular signal-regulated kinase; F = forward; H&E = hematoxylin and eosin stain; HRP = horseradish peroxidase; HS = heat stress; Int = intensity; JAK/STAT = Janus kinase/signal transducers and activators of transcription; MAPK = mitogen-activated protein kinase; MEC = mammary epithelial cell; mTOR = mammalian target of rapamycin; MY = milk yield; NCBI = National Center for Biotechnology Information; pAKT = phosphorylated AKT; PFTN = pair-feeding thermoneutral; PI = propidium iodide; p38MAPK = p38 mitogen-activated protein kinase; Pp38 MAPK = phosphorylated p38 mitogen-activated protein kinase; PRL = prolactin; PRLR = PRL receptor; pSTAT5 = phosphorylated signal transducer and activator of transcription 5; R = reverse; pS6K1 = phosphorylated S6K1; TBST = tris-buffered saline solution with Tween 20; THI = temperature-humidity index; TN = thermoneutral.

REFERENCES

Akers, R. M. 2016. Lactation and the Mammary Gland. John Wiley & Sons.

Andón, F. T., and B. Fadeel. 2013. Programmed cell death: Molecular mechanisms and implications for safety assessment of nanomaterials. Acc. Chem. Res. 46:733–742. https://doi.org/10.1021/ar300020b.

Bach, K., S. Pensa, M. Grzelak, J. Hadfield, D. J. Adams, J. C. Marioni, and W. T. Khaled. 2017. Differentiation dynamics of mammary epithelial cells revealed by single-cell RNA sequencing. Nat. Commun. 8:2128. https://doi.org/10.1038/s41467-017-02001-5.

Baumgard, L. H., and R. P. Rhoads. 2012. Ruminant nutrition symposium: Ruminant production and metabolic responses to heat stress. J. Anim. Sci. 90:1855–1865. https://doi.org/10.2527/jas.2011-4675.

Baumgard, L. H., and R. P. Rhoads Jr.. 2013. Effects of heat stress on postabsorptive metabolism and energetics. Annu. Rev. Anim. Biosci. 1:311–337. https://doi.org/10.1146/annurev-animal-031412-103644.

Ben Chedly, H., P. Lacasse, P. G. Marnet, and M. Boutinaud. 2013. The decrease in milk yield during once daily milking is due to regulation of synthetic activity rather than apoptosis of mammary epithelial cells in goats. Animal 7:124–133. https://doi.org/10.1017/S1751731112001176.

Berchtold, D., and T. C. Walther. 2009. TORC2 plasma membrane localization is essential for cell viability and restricted to a distinct domain. Mol. Biol. Cell 20:1565–1575. https://doi.org/10.1091/mbc.e08-10-1001.

Bernabucci, U., S. Biffani, L. Buggiotti, A. Vitali, N. Lacetera, and A. Nardone. 2014. The effects of heat stress in Italian Holstein dairy cattle. J. Dairy Sci. 97:471–486. https://doi.org/10.3168/jds.2013-6611.

Blatteis, C., J. Boulant, M. Cabanac, B. Cannon, R. Freedman, C. J. Gordon, J. R. S. Hales, M. Horowitz, M. Iriki, and L. Janský. 2001. Glossary of terms for thermal physiology. Jpn. J. Physiol. 51:245–280.

Boutinaud, M., and H. Jammes. 2002. Potential uses of milk epithelial cells: A review. Reprod. Nutr. Dev. 42:133–147. https://doi.org/10.1051/rnd:2002013.

Boutinaud, M., L. Yart, P. Debournoux-Poton, S. Wiart, L. Finot, E. Le Guennec, P.-G. Marnet, F. Dessauge, and V. Lollivier. 2013. Exfoliation of mammary epithelial cells in milk is linked with lactation persistency in dairy cows. 64. Annual Meeting of the European Federation of Animal Science (EAAP). Nantes, France. Wageningen Academic Publishers.

Cai, M., Y. Hu, T. Zheng, H. He, W. Xiao, B. Liu, Y. Shi, X. Jia, S. Chen, J. Wang, and S. Lai. 2018. MicroRNA-216b inhibits heat stress-induced cell apoptosis by targeting Fas in bovine mammary epithelial cells. Cell Stress Chaperones 23:921–931. https://doi.org/10.1007/s12192-018-0899-9.

Capuco, A. V., S. E. Ellis, S. A. Hale, E. Long, R. A. Erdman, X. Zhao, and M. J. Paape. 2003. Lactation persistency: Insights from mammary cell proliferation studies. J. Anim. Sci. 81(Suppl. 3):18–31. https://doi.org/10.2527/2003.81suppl_318x.

Capuco, A. V., D. L. Wood, R. Baldwin, K. Mcleod, and M. J. Paape. 2001. Mammary cell number, proliferation, and apoptosis during a bovine lactation: Relation to milk production and effect of bST. J. Dairy Sci. 84:2177–2187. https://doi.org/10.3168/jds.S0022-0302(01)74664-4.

Chen, K.-L., H.-L. Wang, L.-Z. Jiang, Y. Qian, C.-X. Yang, W.-W. Chang, J.-F. Zhong, and G.-D. Xing. 2020. Heat stress induces apoptosis through disruption of dynamic mitochondrial networks in dairy cow mammary epithelial cells. In Vitro Cell. Dev. Biol. Anim. 56:322–331. https://doi.org/10.1007/s11626-020-00446-5.

Collier, R. J., J. L. Collier, R. P. Rhoads, and L. H. Baumgard. 2008. Invited review: Genes involved in the bovine heat stress response. J. Dairy Sci. 91:445–454. https://doi.org/10.3168/jds.2007-0540.

Cowley, F. C., D. G. Barber, A. V. Houlihan, and D. P. Poppi. 2015. Immediate and residual effects of heat stress and restricted intake on milk protein and casein composition and energy metabolism. J. Dairy Sci. 98:2356–2368. https://doi.org/10.3168/jds.2014-8442.

Dado-Senn, B., A. L. Skibiel, G. E. Dahl, S. I. Arriola Apelo, and J. Laporta. 2021. Dry period heat stress impacts mammary protein metabolism in the subsequent lactation. Animals (Basel) 11:2676. https://doi.org/10.3390/ani11092676.

Dado-Senn, B., A. L. Skibiel, T. F. Fabris, G. E. Dahl, and J. Laporta. 2019. Dry period heat stress induces microstructural changes in the lactating mammary gland. PLoS One 14:e0222120. https://doi.org/10.1371/journal.pone.0222120.

Dado-Senn, B., A. L. Skibiel, T. F. Fabris, Y. Zhang, G. E. Dahl, F. Peñagaricano, and J. Laporta. 2018. RNA-Seq reveals novel genes and pathways involved in bovine mammary involution during the dry period and under environmental heat stress. Sci. Rep. 8:11096. https://doi.org/10.1038/s41598-018-29420-8.

do Amaral, B. C., E. E. Connor, S. Tao, M. J. Hayen, J. W. Bubolz, and G. E. Dahl. 2011. Heat stress abatement during the dry period influences metabolic gene expression and improves immune status in the transition period of dairy cows. J. Dairy Sci. 94:86–96. https://doi.org/10.3168/jds.2009-3004.

Ellett, M. D., R. P. Rhoads, M. D. Hanigan, B. A. Corl, G. Perez-Hernandez, C. L. M. Parsons, L. H. Baumgard, and K. M. Daniels. 2024. Relationships between gastrointestinal permeability, heat stress, and milk production in lactating dairy cows. J. Dairy Sci. 107:5190–5203. https://doi.org/10.3168/jds.2023-24043.

Fabris, T. F., J. Laporta, F. N. Corra, Y. M. Torres, D. J. Kirk, D. J. McLean, J. D. Chapman, and G. E. Dahl. 2017. Effect of nutritional immunomodulation and heat stress during the dry period on subsequent performance of cows. J. Dairy Sci. 100:6733–6742. https://doi.org/10.3168/jds.2016-12313.

Fabris, T. F., J. Laporta, A. L. Skibiel, F. N. Corra, B. D. Senn, S. E. Wohlgemuth, and G. E. Dahl. 2019. Effect of heat stress during early, late, and entire dry period on dairy cattle. J. Dairy Sci. 102:5647–5656. https://doi.org/10.3168/jds.2018-15721.

Fabris, T. F., J. Laporta, A. L. Skibiel, B. Dado-Senn, S. E. Wohlgemuth, and G. E. Dahl. 2020. Effect of heat stress during the early and late dry period on mammary gland development of Holstein dairy cattle. J. Dairy Sci. 103:8576–8586. https://doi.org/10.3168/jds.2019-17911.

Fan, C., R. Hu, H. Fan, Y. Yang, B. Gong, S. Zhang, J. Ding, Y. Su, Z. Zhuo, and J. Cheng. 2021. Effects of seasonal ambient heat stress on expression of microRNAs in the mammary gland of Holstein cows. Int. J. Biometeorol. 65:235–246. https://doi.org/10.1007/s00484-020-02025-5.

Feugeas, J.-P., J. Tourret, A. Launay, O. Bouvet, C. Hoede, E. Denamur, and O. Tenaillon. 2016. Links between transcription, environmental adaptation and gene variability in *Escherichia coli*: Correlations between gene expression and gene variability reflect growth efficiencies. Mol. Biol. Evol. 33:2515–2529. https://doi.org/10.1093/molbev/msw105.

Ganger, M. T., G. D. Dietz, and S. J. Ewing. 2017. A common base method for analysis of qPCR data and the application of simple blocking in qPCR experiments. BMC Bioinformatics 18:534. https://doi.org/10.1186/s12859-017-1949-5.

Gao, S. T., J. Guo, S. Y. Quan, X. M. Nan, M. S. Fernandez, L. H. Baumgard, and D. P. Bu. 2017. The effects of heat stress on protein metabolism in lactating Holstein cows. J. Dairy Sci. 100:5040–5049. https://doi.org/10.3168/jds.2016-11913.

Gao, S. T., L. Ma, Z. Zhou, Z. K. Zhou, L. H. Baumgard, D. Jiang, M. Bionaz, and D. P. Bu. 2019. Heat stress negatively affects the transcriptome related to overall metabolism and milk protein synthesis in mammary tissue of midlactating dairy cows. Physiol. Genomics 51:400–409. https://doi.org/10.1152/physiolgenomics.00039.2019.

García Solá, M. E., M. Stedile, I. Beckerman, and E. C. Kordon. 2021. An integrative single-cell transcriptomic atlas of the post-natal mouse mammary gland allows discovery of new developmental trajectories in the luminal compartment. J. Mammary Gland Biol. Neoplasia 26:29–42. https://doi.org/10.1007/s10911-021-09488-1.

Hammami, H., J. Vandenplas, M.-L. Vanrobays, B. Rekik, C. Bastin, and N. Gengler. 2015. Genetic analysis of heat stress effects on yield traits, udder health, and fatty acids of Walloon Holstein cows. J. Dairy Sci. 98:4956–4968. https://doi.org/10.3168/jds.2014-9148.

Herve, L., H. Quesnel, V. Lollivier, and M. Boutinaud. 2016. Regulation of cell number in the mammary gland by controlling the exfoliation process in milk in ruminants. J. Dairy Sci. 99:854–863. https://doi.org/10.3168/jds.2015-9964.

Herve, L., H. Quesnel, M. Veron, J. Portanguen, J. J. Gross, R. M. Bruckmaier, and M. Boutinaud. 2019. Milk yield loss in response to feed restriction is associated with mammary epithelial cell exfoliation in dairy cows. J. Dairy Sci. 102:2670–2685. https://doi.org/10.3168/jds.2018-15398.

Hu, H., Y. Zhang, N. Zheng, J. Cheng, and J. Wang. 2016. The effect of heat stress on gene expression and synthesis of heat-shock and milk proteins in bovine mammary epithelial cells. Anim. Sci. J. 87:84–91. https://doi.org/10.1111/asj.12375.

Kakumoto, K., J. Ikeda, M. Okada, E. Morii, and C. Oneyama. 2015. mLST8 promotes mTOR-mediated tumor progression. PLoS One 10:e0119015. https://doi.org/10.1371/journal.pone.0119015.

Key, N., S. Sneeringer, and D. Marquardt. 2014. Climate change, heat stress, and U.S. dairy production. USDA-ERS Econ. Res. Rep. No. ERR-175. Accessed Jan. 18, 2023. https://www.ers.usda.gov/webdocs/publications/45279/49164_err175.pdf?v=7392.7.

Kobayashi, K., Y. Tsugami, K. Matsunaga, T. Suzuki, and T. Nishimura. 2018. Moderate high temperature condition induces the lactation capacity of mammary epithelial cells through control of STAT3 and STAT5 signaling. J. Mammary Gland Biol. Neoplasia 23:75–88. https://doi.org/10.1007/s10911-018-9393-3.

Krishna, M., and H. Narang. 2008. The complexity of mitogen-activated protein kinases (MAPKs) made simple. Cell. Mol. Life Sci. 65:3525–3544. https://doi.org/10.1007/s00018-008-8170-7.

Lacetera, N., U. Bernabucci, D. Scalia, L. Basiricò, P. Morera, and A. Nardone. 2006. Heat stress elicits different responses in peripheral blood mononuclear cells from Brown Swiss and Holstein cows. J. Dairy Sci. 89:4606–4612. https://doi.org/10.3168/jds.S0022-0302(06)72510-3.

Lecchi, C., N. Rota, A. Vitali, F. Ceciliani, and N. Lacetera. 2016. In vitro assessment of the effects of temperature on phagocytosis, reactive oxygen species production and apoptosis in bovine polymorphonuclear cells. Vet. Immunol. Immunopathol. 182:89–94. https://doi.org/10.1016/j.vetimm.2016.10.007.

Lengi, A. J., M. Makris, and B. A. Corl. 2021. A flow cytometric method for measuring and isolating mammary epithelial cells from bovine milk. JDS Commun. 2:426–430. https://doi.org/10.3168/jdsc.2021-0135.

Lengi, A. J., J. W. Stewart, M. Makris, M. L. Rhoads, and B. A. Corl. 2022. Heat stress increases mammary epithelial cells and reduces viable immune cells in milk of dairy cows. Animals (Basel) 12:2810. https://doi.org/10.3390/ani12202810.

Li, L., Y. Wang, C. Li, and G. Wang. 2017. Proteomic analysis to unravel the effect of heat stress on gene expression and milk synthesis in bovine mammary epithelial cells. Anim. Sci. J. 88:2090–2099. https://doi.org/10.1111/asj.12880.

Li, Y., G. Chen, S. Xu, S. Xia, W. Sun, J. Wang, S. Chen, S. Lai, and X. Jia. 2024. miR-425–5p regulates proliferation of bovine mammary epithelial cells by targeting TOB2. Genes (Basel) 15:174. https://doi.org/10.3390/genes15020174.

Lollivier, V., P. Lacasse, J. Angulo Arizala, P. Lamberton, S. Wiart, J. Portanguen, R. Bruckmaier, and M. Boutinaud. 2015. In vivo inhibition followed by exogenous supplementation demonstrates galactopoietic effects of prolactin on mammary tissue and milk production in dairy cows. J. Dairy Sci. 98:8775–8787. https://doi.org/10.3168/jds.2015-9853.

Martin Carli, J. F., G. D. Trahan, and M. C. Rudolph. 2021. Resolving human lactation heterogeneity using single milk-derived cells, a resource at the ready. J. Mammary Gland Biol. Neoplasia 26:3–8. https://doi.org/10.1007/s10911-021-09489-0.

Motyl, T., M. Gajewska, J. Zarzynska, A. Sobolewska, and B. Gajkowska. 2007. Regulation of autophagy in bovine mammary epithelial cells. Autophagy 3:484–486. https://doi.org/10.4161/auto.4491.

NRC. 2001. Nutritional Requirements of Dairy Cattle. 7th rev. ed. National Academies Press.

Ouellet, V., I. M. Toledo, B. Dado-Senn, G. E. Dahl, and J. Laporta. 2021. Critical temperature-humidity index thresholds for dry cows in a subtropical climate. Front. Anim. Sci. 2:706636. https://doi.org/10.3389/fanim.2021.706636.

Pearson, G., F. Robinson, T. Beers Gibson, B. E. Xu, M. Karandikar, K. Berman, and M. H. Cobb. 2001. Mitogen-activated protein (MAP) kinase pathways: Regulation and physiological functions. Endocr. Rev. 22:153–183. https://doi.org/10.1210/edrv.22.2.0428.

Ravagnolo, O., I. Misztal, and G. Hoogenboom. 2000. Genetic component of heat stress in dairy cattle, development of heat index function. J. Dairy Sci. 83:2120–2125. https://doi.org/10.3168/jds.S0022-0302(00)75094-6.

Rhoads, M. L., R. P. Rhoads, M. J. VanBaale, R. J. Collier, S. R. Sanders, W. J. Weber, B. A. Crooker, and L. H. Baumgard. 2009. Effects of heat stress and plane of nutrition on lactating Holstein cows: I. Production, metabolism, and aspects of circulating somatotropin. J. Dairy Sci. 92:1986–1997. https://doi.org/10.3168/jds.2008-1641.

Schwanhäusser, B., D. Busse, N. Li, G. Dittmar, J. Schuchhardt, J. Wolf, W. Chen, and M. Selbach. 2011. Global quantification of mammalian gene expression control. Nature 473:337–342. https://doi.org/10.1038/nature10098.

Silanikove, N., F. Shapiro, and D. Shinder. 2009. Acute heat stress brings down milk secretion in dairy cows by up-regulating the activity of the milk-borne negative feedback regulatory system. BMC Physiol. 9:13. https://doi.org/10.1186/1472-6793-9-13.

Sirka, O. K., E. R. Shamir, and A. J. Ewald. 2018. Myoepithelial cells are a dynamic barrier to epithelial dissemination. J. Cell Biol. 217:3368–3381. https://doi.org/10.1083/jcb.201802144.

Skibiel, A. L., F. Peñagaricano, R. Amorín, B. M. Ahmed, G. E. Dahl, and J. Laporta. 2018. In utero heat stress alters the offspring epigenome. Sci. Rep. 8:14609. https://doi.org/10.1038/s41598-018-32975-1.

Smith, D. L., T. Smith, B. J. Rude, and S. H. Ward. 2013. Short communication: Comparison of the effects of heat stress on milk and component yields and somatic cell score in Holstein and Jersey cows. J. Dairy Sci. 96:3028–3033. https://doi.org/10.3168/jds.2012-5737.

Smith, S. 1994. The animal fatty acid synthase: One gene, one polypeptide, seven enzymes. FASEB J. 8:1248–1259. https://doi.org/10.1096/fasebj.8.15.8001737.

Sonna, L. A., J. Fujita, S. L. Gaffin, and C. M. Lilly. 2002. Invited review: Effects of heat and cold stress on mammalian gene expression. J. Appl. Physiol. 92:1725–1742. https://doi.org/10.1152/japplphysiol.01143.2001.

Spiers, D. E., J. N. Spain, J. D. Sampson, and R. P. Rhoads. 2004. Use of physiological parameters to predict milk yield and feed intake in heat-stressed dairy cows. J. Therm. Biol. 29:759–764. https://doi.org/10.1016/j.jtherbio.2004.08.051.

St-Pierre, N. R., B. Cobanov, and G. Schnitkey. 2003. Economic losses from heat stress by US livestock industries. J. Dairy Sci. 86:E52–E77. https://doi.org/10.3168/jds.S0022-0302(03)74040-5.

Stefanon, B., M. Colitti, G. Gabai, C. H. Knight, and C. J. Wilde. 2002. Mammary apoptosis and lactation persistency in dairy animals. J. Dairy Res. 69:37–52. https://doi.org/10.1017/S0022029901005246.

Tao, S., J. W. Bubolz, B. C. do Amaral, I. M. Thompson, M. J. Hayen, S. E. Johnson, and G. E. Dahl. 2011. Effect of heat stress during the dry period on mammary gland development. J. Dairy Sci. 94:5976–5986. https://doi.org/10.3168/jds.2011-4329.

Tao, S., A. P. A. Monteiro, I. M. Thompson, M. J. Hayen, and G. E. Dahl. 2012. Effect of late-gestation maternal heat stress on growth and immune function of dairy calves. J. Dairy Sci. 95:7128–7136. https://doi.org/10.3168/jds.2012-5697.

Tao, S., R. M. Orellana, X. Weng, T. N. Marins, G. E. Dahl, and J. K. Bernard. 2018. Symposium review: The influences of heat stress on bovine mammary gland function. J. Dairy Sci. 101:5642–5654. https://doi.org/10.3168/jds.2017-13727.

Wakasa, H., Y. Tsugami, T. Koyama, L. Han, T. Nishimura, N. Isobe, and K. Kobayashi. 2022. Adverse effects of high temperature on mammary alveolar development in vitro. J. Mammary Gland Biol. Neoplasia 27:155–170. https://doi.org/10.1007/s10911-022-09518-6.

Watson, C. J., and T. G. Burdon. 1996. Prolactin signal transduction mechanisms in the mammary gland: The role of the Jak/Stat pathway. Rev. Reprod. 1:1–5. https://doi.org/10.1530/ror.0.0010001.

Weng, X., A. P. A. Monteiro, J. Guo, C. Li, R. M. Orellana, T. N. Marins, J. K. Bernard, D. J. Tomlinson, J. M. DeFrain, S. E. Wohlgemuth, and S. Tao. 2018. Effects of heat stress and dietary zinc source on performance and mammary epithelial integrity of lactating dairy cows. J. Dairy Sci. 101:2617–2630. https://doi.org/10.3168/jds.2017-13484.

West, J. W., B. G. Mullinix, and J. K. Bernard. 2003. Effects of hot, humid weather on milk temperature, dry matter intake, and milk yield of lactating dairy cows. J. Dairy Sci. 86:232–242. https://doi.org/10.3168/jds.S0022-0302(03)73602-9.

Wheelock, J. B., R. P. Rhoads, M. J. VanBaale, S. R. Sanders, and L. H. Baumgard. 2010. Effects of heat stress on energetic metabolism in lactating Holstein cows. J. Dairy Sci. 93:644–655. https://doi.org/10.3168/jds.2009-2295.

Wohlgemuth, S. E., Y. Ramirez-Lee, S. Tao, A. P. A. Monteiro, B. M. Ahmed, and G. E. Dahl. 2016. Short communication: Effect of heat

stress on markers of autophagy in the mammary gland during the dry period. J. Dairy Sci. 99:4875–4880. https://doi.org/10.3168/jds.2015-10649.
Xie, F., P. Xiao, D. Chen, L. Xu, and B. Zhang. 2012. miRDeepFinder: A miRNA analysis tool for deep sequencing of plant small RNAs. Plant Mol. Biol. 80:75–84. https://doi.org/10.1007/s11103-012-9885-2.
Yue, S., Z. Wang, L. Wang, Q. Peng, and B. Xue. 2020. Transcriptome functional analysis of mammary gland of cows in heat stress and thermoneutral condition. Animals (Basel) 10:1015. https://doi.org/10.3390/ani10061015.
Zhao, F.-Q. 2014. Biology of glucose transport in the mammary gland. J. Mammary Gland Biol. Neoplasia 19:3–17. https://doi.org/10.1007/s10911-013-9310-8.
Zhao, F.-Q., P. J. Miller, E. H. Wall, Y.-C. Zheng, B. Dong, M. C. Neville, and T. B. McFadden. 2004. Bovine glucose transporter GLUT8: Cloning, expression, and developmental regulation in mammary gland. Biochim. Biophys. Acta 1680:103–113.
Zimbelman, R. B., R. J. Collier, and M. L. Eastridge. 2011. Feeding strategies for high-producing dairy cows during periods of elevated heat and humidity. Pages 111–126 in Tri-State Dairy Nutrition Conference, Fort Wayne, IN.
Zimbelman, R. B., R. P. Rhoads, M. L. Rhoads, G. C. Duff, L. H. Baumgard, and R. J. Collier. 2009. A re-evaluation of the impact of temperature humidity index (THI) and black globe humidity index (BGHI) on milk production in high producing dairy cows. Pages 158–169 in Proceedings of the Southwest Nutrition Conference. R. J. Collier, ed.

ORCIDS

G. Perez-Hernandez https://orcid.org/0000-0001-6814-2927
M. D. Ellett https://orcid.org/0000-0002-0112-6532
L. J. Banda https://orcid.org/0000-0003-4104-6841
A. J. Lengi https://orcid.org/0000-0002-6200-8185
K. M. Daniels https://orcid.org/0000-0002-1437-1457
B. A. Corl https://orcid.org/0000-0002-6495-3279